analytical chemistry

pubs.acs.org/ac

Technical Note

Merging Lateral Flow Immunoassay with Electroanalysis as a Novel Sensing Platform: Prostate Specific Antigen Detection as Case of Study

Antonella Miglione, Fabio Di Nardo,* Simone Cavalera, Thea Serra, Claudio Baggiani, Stefano Cinti,* and Laura Anfossi

Cite This: https://doi.org/10.1021/acs.analchem.3c04078

Read Online

ABSTRACT: The COVID-19 pandemic highlighted lateral flow immunoassay (LFIA) strips as the most known point-of-care (POC) devices enabling rapid and easy detection of relevant biomarkers by nonspecialists. However, these diagnostic tests are usually associated with the qualitative detection of the biomarker of interest. Alternatively, electrochemical-based diagnostics, especially known for diabetes care, enable quantitative determination of biomarkers. From an analytical point perspective, the combination of the two approaches might represent a step forward for the POC world: in fact, electrochemical transduction is attractive to be integrated into LFIA strips due to its simplicity, high sensitivity, fast signal generation, and cost effectiveness. In this work, a LFIA strip has been combined with an electrochemical transduction, yielding an electrochemical LFIA (eLFIA). As a proof-of-concept method, the detection of prostate-specific antigen has been carried out by combining a printed-electrochemical strip with the traditional LFIA tests. The electrochemical detection has been based on the measurement of Au ions produced from the dissolution of the gold nanoparticles previously captured on the test line. The analytical performances obtained at LFIA and eLFIA were compared, highlighting how the use of differential pulse voltammetry allowed for a lower detection limit (2.5-fold), respectively, 0.38 and 0.15 ng/mL, but increasing the time of analysis. Although the correlation between the two architectures confirmed the satisfactory agreement of outputs, this technical note has been thought to provide the reader a fair statement with regard to the strength and drawbacks about combining the two (apparently) competitor devices in a diagnostics field, namely, LFIA and electrochemical strips.

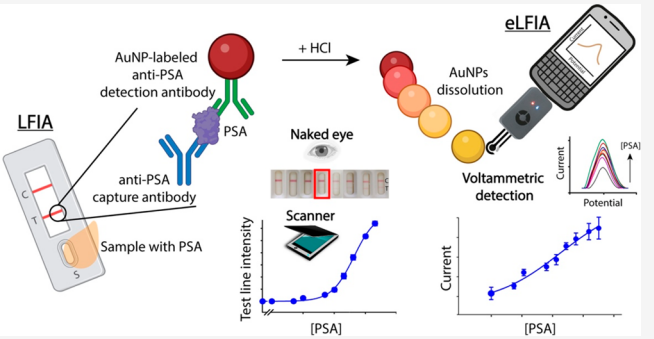

The lateral flow immunoassays (LFIAs) satisfy the criteria of an "ASSURED" point-of-care (POC) device (Affordable, Sensitive, Specific, User-friendly, Rapid and robust, Equipment-free, and Delivered to the end-users)[1] and can easily address also the additional requirements recently introduced with the REASSURED criteria (real-time connectivity, ease of specimen collection, and environmental friendliness).[2] Some of the key features of LFIAs are the possibility to (1) perform quick analysis, e.g., 5−30 min, (2) require a one-step procedure without any additional equipment, and (3) be low cost.[3] However, the simplest LFIAs only provide a qualitative result regarding the presence or absence of the target analyte, and sensitivity and specificity are often worse if compared to lab-based tests.[4]

In the last few decades, huge efforts have been made to improve the analytical performances of the traditional LFIAs. Several strategies have been studied and reported, such as the chemical enhancement to improve the signal/background ratio in the test line,[5] the use of readers, and the adoption of different transduction systems, i.e., fluorescence,[6] chemiluminescence,[7] surface-enhanced Raman scattering (SERS),[8] photothermal,[9] etc. It should be noted that, even if these strategies have clearly improved the traditional LFIAs, the resulting procedures have been made more complex, time consuming, and expensive.

Among the various sensing and biosensing architectures, electrochemical architectures represent promising candidates to be coupled with LFIAs. In fact, the adoption of electroanalytical methods has highlighted the possibility to be coupled with several decentralized settings, from wearable to implantable devices.[10] The effectiveness of electroanalytical systems is associated with the easiness in miniaturization and

Received: September 11, 2023
Revised: January 3, 2024
Accepted: January 8, 2024

the possibility to analyze colored/turbid matrices.[11] The interest toward the implementation of miniaturized and low-cost electrochemical readers is growing. Several companies are currently producing smartphone-based potentiostats with the adoption of user-friendly software. It should be noted that the electroanalytical systems would represent an excellent alternative to existing solutions (e.g., fluorescence, chemiluminescence, SERS, etc.) to be combined with LFIAs for making these more sensitive, without adopting complicated setups. However, despite the aforementioned unique features, electrochemical-supported LFIA (eLFIA) still represents a niche,[12] and recently published reviews have highlighted some applications toward this vision, by merging the advantages of a LFIA with those of the electrochemical detection.[13,14] The complete coupling of electroanalysis to LFIA is still an open challenge mostly due to the requirements of complicated experimental setups that might hinder their future commercialization. Although many approaches have been reported including the use of both biological and inorganic labels, e.g., horseradish peroxidase and quantum dots,[15,16] the ex situ detection which involves the electrochemical detection after cutting the test line zone appears as the most feasible route. The use of gold nanoparticles (AuNPs) as transduction labels is often preferred for their double colorimetric/electrochemical readout. It should be considered that commercially available LFIAs are mainly manufactured with these labels[12] that have been also highlighted in electroanalysis detection due to their increasing relevance and use as antimicrobial and therapeutic agents.[17] Our idea has involved the combination of naked-eye detection with electrochemical quantification by dissolving the AuNPs captured on the test line and then measuring Au ions at the working electrode. To date, a unique example has been reported in the literature based on a similar dissolution of AuNPs from LFIA. However, the AuNPs dissolution step was complicated (a HBr−Br_2 mixture dissolves AuNPs, and the following addition of phenoxyacetic acid eliminates the excess of Br_2 before the analysis). Also, the use of a traditional bulk electrode was not compatible with a portable application, and the electrochemical detection only replaced the naked-eye one.

In this technical note, we report for the first time a whole decentralized platform for the use of nonspecialists, by empowering a classical AuNP-based LFIA with electrochemical detection at smartphone-powered portable potentiostat. As the case of study, the proposed eLFIA has been applied toward the detection of the prostate specific antigen (PSA), commonly used for prostate cancer early diagnosis and therapy management.[18] It should be considered that colorimetric LFIA is usually coupled with the use of a scanner to improve the analytical performance. Herein, to provide a frugal alternative, a vial was prefilled with a few microliters of hydrochloric acid, which allowed the AuNPs to be dissolved and detected. Specifically, the end-user is only asked to perform the LFIA, insert the test line, add water into the vial, and read the electrochemical readout on the smartphone. Both optical and electrochemical readings have been performed, characterized, and correlated, demonstrating that electroanalysis is not going to replace naked-eye visualization but is able to provide a complementary analytical tool without adding experimental tasks. The ease of the approach, supported by miniaturization, might represent the starting point for plenty of applications, maintaining the cost effectiveness and the portability requirement for point-of-care testing.

EXPERIMENTAL SECTION

(Bio)reagents, Chemicals, Materials, And Software. Gold(III) chloride trihydrate (ACS reagent), antimouse immunoglobulin G antibody produced in goat, boric acid, sodium tetraborate decahydrate, casein sodium salt from milk, sucrose, bovine serum albumin (BSA), hydrochloric acid, and commercial AuNPs were obtained from Sigma−Aldrich (St. Louis, MO, USA). Tween 20, sodium chloride, sodium dihydrogen phosphate, and disodium hydrogen phosphate were purchased from VWR International (Milan, Italy). Nitrocellulose membranes (CNPC-SS12) with a cellulose absorbent pad and FR-1 sample pads were purchased by Advanced Microdevices Pvt. Ltd. (Ambala, India). Glass fiber conjugate pads were obtained from Merck Millipore (Billerica, MA, USA). The anti-PSA monoclonal antibody (mAb_1) used to form the test line was purchased from Fitzgerald Industries International (North Acton, MA, USA), while the anti-PSA mAb used for AuNPs conjugates and the PSA used to prepare the standard solutions were provided by NIB biotec Srl (Torino, Italy). SigmaPlot v.14.0 (Systat Software, Inc.) was used to perform the statistical analyses. The strip images were acquired by a benchtop scanner (OpticSlim 550 scanner, Plustek Technology GmbH, Norderstedt, Germany) and processed by QuantiScan 3.0 software (Biosoft, Cambridge, UK) to obtain the signal intensities. For the electrochemical detection, a Sensit Smart (Palmsens, The Netherlands) small wireless potentiostat connected to a smartphone was employed.

Preparation and Characterization of AuNPs and Anti-PSA mAb-AuNPs Conjugate. AuNPs with a mean diameter of 30 nm were synthesized through tetrachloroauric acid reduction with sodium citrate, as previously reported.[19,20] Very briefly, 1 mL of 1% w/v sodium citrate was added to 100 mL of boiling 0.01% w/v tetrachloroauric acid under vigorous stirring. After a few seconds, the color turned to ruby red (indicating successful formation of AuNPs), and it was kept boiling for 5 min. Finally, the AuNPs were cooled to room temperature and stored at 4 °C for successive conjugation to anti-PSA mAb. AuNPs were characterized by UV−vis spectroscopy on a Cary 60 UV−vis spectrophotometer (Agilent Technologies, USA) and by transmission electron microscopy using a Jeol 3010-UHR (Jeol Ltd., Japan) high resolution transmission electron microscope (HR-TEM) equipped with a LaB6 filament operating at 300 kV. The AuNP resulted almost spherical in shape, with a sharp SPR band centered at 525 nm (Figure S1).

The AuNPs-Ab anti-PSA (AuNPs-Ab) conjugate was prepared by passive adsorption of anti-PSA mAb on the surface of the AuNPs. Briefly, the AuNPs pH was adjusted to ∼8.5 with carbonate buffer (0.05 M, pH 9.6). Then, for each milliliter of AuNPs with optical density (OD) 1, the appropriate amount of the mAb was added and gently mixed for 30 min at 37 °C. Subsequently, 100 μL of blocking solution (borate buffer supplemented with 1% w/v casein) was added (for each milliliter of AuNPs) to block the unbound sites for 10 min at 37 °C. Finally, the AuNPs-mAb conjugate was recovered by centrifugation (10 min at 7100*g*), washed twice with borate buffer supplemented with 0.1% casein, and reconstituted in borate buffer supplemented with 2% (w/v) sucrose, 1% (w/v) casein, 0.25% (v/v) Tween 20, and 0.02% (w/v) NaN_3. AuNPs-mAb conjugates were stored at 4 °C until use. The appropriate amount of mAb to be added to obtain

https://doi.org/10.1021/acs.analchem.3c04078
Anal. Chem. XXXX, XXX, XXX−XXX

stable conjugates was evaluated through the flocculation stress test.[20] According to the flocculation stress test, the minimum amount to obtain stable conjugate was 6 μg of mAb per 1 mL of AuNPs (Figure S2).

LFIA Strip Manufacturing. The mAb_1 (0.5 mg/mL) and goat antimouse IgG (0.5 mg/mL) diluted in phosphate buffer (20 mM, pH 7.4) were spotted onto NC membranes at 1 μL/cm by means of an XYZ3050 platform (Biodot, Irvine, CA, USA) to form the test and control lines, respectively. The fine-tuning of the test line concentration is reported in Figure S3. The conjugate pad was presaturated with borate buffer supplemented with 2% (w/v) sucrose, 1% (w/v) BSA, 0.25% (v/v) Tween 20, and 0.02% (w/v) NaN_3 and dried at 60 °C for 1 h. Subsequently, AuNPs-Ab conjugate solution at OD 0.25 (80 μL/cm) was used to saturate the conjugate pad. Then, it was dried at room temperature for 3 h. The NC membranes were dried at 37 °C for 60 min under vacuum, layered with sample and conjugate pads, cut into 3.5 mm wide strips by means of a CM4000 guillotine (Biodot), and inserted into plastic cassettes (Kinbio, Shanghai, China) to fabricate the ready-to-use LFA device. Cassettes were stored in the dark in plastic bags containing silica at room temperature until use.

SPE Manufacturing. Screen-printed electrodes were manufactured by serigraphy. Autostat HT5 polyester sheets were used as a flexible support. Ag/AgCl (Elettrodag 477 SS) ink has been used to print the reference electrode, while graphite-based conductive ink (Elettrodag 421) has been used for printing both the working and counter electrode.[21] After each printing step, the electrodes have been cured in the oven for 20 min at 80 °C. The area of the electrochemical cell has been defined by using adhesive tape also avoiding samples reaching the electrical connectors at the potentiostat. The final diameter of the working electrode is 4 mm.

Assay Principle. The principle of the proposed eLFIA is depicted in Figure 1.

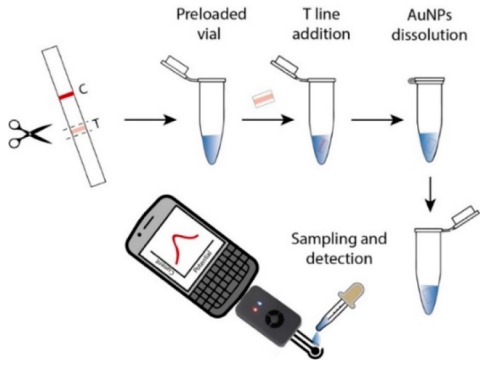

Figure 1. Experimental setup of eLFIA architecture which includes LFIA visualization, cutting of the test line, AuNPs dissolution in preacidified vials, and smartphone-based electrochemical detection.

The sensing concept is to exploit the AuNPs for both colorimetric and electrochemical detections, depending on the analytical need. To start the assay, 70 μL of PSA standard solutions (concentration ranged from 0 to 20 ng/mL, prepared in 20 mM phosphate buffer, pH 7.4, supplemented with 1% w/v BSA and 0.1% v/v Tween 20) was applied to the sample pad. When the sample containing the PSA reaches the conjugate pad, the enzyme interacts with the AuNPs-Ab forming a first immunocomplex, AuNPs-Ab-PSA. Then, the immunocomplex continues to flow through the NC membrane encountering the capturing anti-PSA mAb in the test line, forming a colored line corresponding to the sandwich immunocomplex AuNPs-Ab-PSA-Ab. The excess of AuNPs-Ab continues to move to the control line, where it is captured by the goat antimouse IgG, forming a second colored line. Thus, in the presence of the target analyte, the colorimetric response results in the formation of two colored lines where the color intensity of the test line is directly proportional to the PSA content in the sample. Instead, in the absence of PSA (or for concentrations lower than the limit of detection), only the control line is visible. After LFIA completion (15 min), both the test and control lines have been cut using common scissors. Successively, the selected line has been introduced into a preloaded vial containing 100 μL of 12 M HCl (it should be noted that the handling for end-user is completely avoided). This step is essential to dissolve all of the AuNPs that have been accumulated onto the chosen line. The process of dissolution takes 3 min. Subsequently, the acidic solution is 10-fold diluted with distilled water to a final concentration of 1 M HCl, and 100 μL is placed onto the electrochemical printed strip to be analyzed with a portable potentiostat coupled to a smartphone. The measurements have been performed through the adoption of differential pulse voltammetry (DPV) using the following parameters: (1) E dep, 1.25 V; t dep, 120 s; E step, 0.01 V; E pulse, 0.2 V; t pulse, 0.02 s; scan rate, 0.05 V/s and (2) E beg, 0.7 V; E end, 0 V; E step, 0.01 V; E pulse, 0.2 V; t pulse, 0.02 s; scan rate, 0.05 V/s.

RESULTS AND DISCUSSION

AuNPs Detection at Portable Electroanalytical Strip. The development of an electroanalytical-based methodology to be combined with the LFIA is based on the determination of the AuNPs that are accumulated on both the test and control lines on the strip. In agreement with the literature, the electrochemical determination is usually performed in hydrochloric solution, as per metal sensing in general. To this regard, the first investigation was about the selection of the acidic media: hydrochloric acid at different concentrations was compared with the use of aqua regia (hydrochloric acid/nitric acid in a 3/1 ratio), using a printed electroanalytical strip for sensing (Figure 2). Among the 0.1 and 1 M HCl and aqua regia, the 1 M HCl was consistent with an optimal recorded signal. In addition, the use of aqua regia might represent a drawback for the dissolution of the silver-based conductive ink used for the screen-printing process. Subsequently, some electrochemical parameters, including the open circuit time

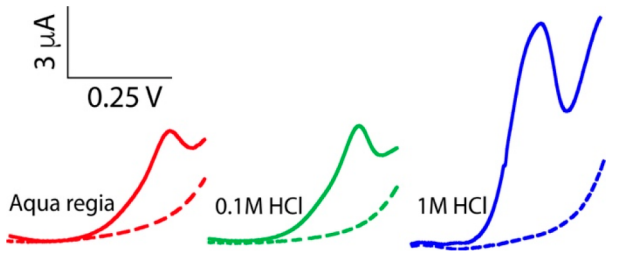

Figure 2. Selection of acidic media to detect AuNPs. Measurements were carried out in the presence of 1 μM AuNPs in aqua regia HCl/HNO_3 (3:1, v/v) (red line), 0.1 M HCl (green line), and 1 M HCl (blue line). The dashed lines are representative of the measurements in absence of AuNPs, and the DPV is performed from 0.5 to 1 V, with a scan rate of 0.1 V/s.

https://doi.org/10.1021/acs.analchem.3c04078
Anal. Chem. XXXX, XXX, XXX−XXX

and the deposition time of the differential pulse voltammetry, have been considered. The open circuit time is about a short period of time where the sample drop is left onto the working electrode surface without applying any potential difference, and it is necessary to have the gold ions physically accumulated.

According to experimental results, 2 min appears as the optimal time to accumulate gold ions at the electrode, while an electrochemical deposition time of 3 min was chosen as the optimal one, also considering that 5 min did not represent a significant improvement of signal intensity to justify almost the double of the time (Figure S4). Considering these preliminary observations, these results have been used as the basis to be applied toward the detection of AuNPs accumulated onto a lateral flow strip.

Analytical Performances of the eLFIA. Depending on the sensing architectures and settings, three different levels of detection can be provided to the end-user. Two main settings should be considered, namely, LFIA and eLFIA. Among these, the LFIA-based detection is capable of offering two levels of sensitivity. In fact, the sensitivity can be estimated through the naked eye observation and by measuring the AuNPs signal intensities from the acquired strip images with the help of a reader (e.g., scanner). Instead, with regard to the eLFIA architecture, sensitivity of the method is estimated through the electrochemical measurement of the Au ions produced from the dissolution of the AuNPs captured on the test line. As reported in Figure 3, the three methods have been reported by interrogating the portable platforms with PSA in the range between 0.01 and 20 ng/mL.

The visual limit of detection (visual LOD) was defined as the lowest PSA concentration resulting in a test line color visible to at least five different operators; as shown in the inset of Figure 3A, it was equal to 1 ng/mL. With regard to the other two settings, namely, LFIA aided by scanner reader and eLFIA, the calibration curves were obtained fitting data with a four-parameter logistic equation. The LOD was calculated as follows: average of the signal at the lowest detectable PSA concentration +3 × standard deviation. The calculated LODs were 0.38 and 0.15 ng/mL, respectively, for LFIA and eLFIA. A 2.5-fold decrease in the LOD may appear as a slight improvement; however, the eLFIA measurements have been performed using nine different homemade SPE for each calibration point, and this could explain the higher imprecision observed. In this proof-of-concept method, we did not modify the electrode, but this would be a strategy to further improve the detectability levels. Repeatability and reproducibility have been evaluated by analyzing PSA standard solutions in triplicate in the same day and in three different days obtaining CV% ≤ 9% for the LFIA (except for 0.1 ng/mL PSA that has CV% equal to 16%) and CV% of ca. 12% for the eLFIA (using nine replicates). However, although the electrochemical detection allowed for lower detection limit, it should be considered that the whole process (which also includes line cutting, dissolution, and electrochemical protocol) makes the PSA measurements ca. 10 min longer with respect to the traditional scanner-aided LFIA ones. However, the two approaches should be seen as complementary in terms of needs of application/sensitivity: one can decide if the electrochemical reader would be preferred to the optical one, and vice versa, depending on the analytical need. In fact, as reported in Figure 4, the correlation between the two approaches has been evaluated: eight randomized strips considering both control and test lines have been measured

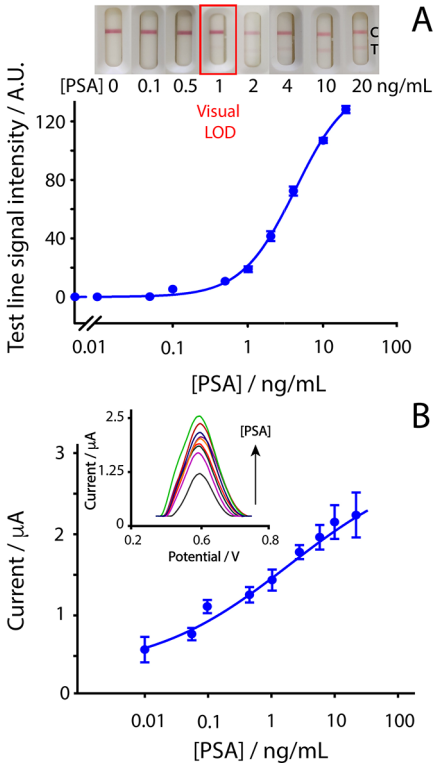

Figure 3. (A) Calibration curve obtained by measuring PSA in the 0.01−20 ng/mL range with the use of a scanner for optical detection. T line average signal and standard deviation is reported (n = 3). Inset: LFIA strips showing the visual LOD (naked-eye detection) equal to 1 ng/mL. (B) Calibration curve obtained by measuring PSA in the 0.01−20 ng/mL range with the use of smartphone-powered potentiostat, namely, eLFIA (n = 9). Inset: Voltammetric curves related to increasing level of PSA.

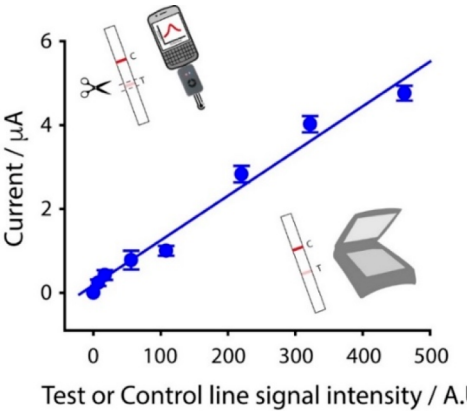

Figure 4. Correlation between eLFIA and LFIA measurements of eight randomized strips for PSA analysis, including both control and test lines (all measurements are in triplicate).

with the two approaches (in triplicate) obtaining a satisfactory coefficient R of 0.985.

CONCLUSION

A common LFIA test has been combined with electrochemical detection through the adoption of a printed strip connected to a smartphone, namely, eLFIA. Although the LFIA tests represent a powerful class of POC devices for the use of nonspecialists in a decentralized context, e.g., pregnancy,

https://doi.org/10.1021/acs.analchem.3c04078
Anal. Chem. XXXX, XXX, XXX−XXX

COVID-19, etc., the aim of this technical note was to provide the reader an easy way to improve the "quantification" feature of these analytical tools. To do this, a smartphone-powered electrochemical assay has been integrated with an LFIA test, using PSA detection as a model study. The electrochemical visualization has been carried out through the use of printed strip following the dissolution of AuNPs in preacidified vials. As per our findings, the addition of the voltammetric measurements allowed us to enhance the sensitivity toward PSA with respect to the use of a scanner commonly employed for the optical visualization (ca. 2.5-fold). The features of eLFIA can be summarized as follows: (1) Cutting the test line and analyzing it into a preacidified vial is user friendly. (2) The electrochemical settings are capable to obtain a lower detection limit if compared to traditional LFIA. (3) The electrochemical combination is characterized by an additional 10 min of analysis, making the entire system slower than the traditional LFIA. However, eLFIA should not be seen as a replacement of LFIA, instead as a complementary tool: depending on the sensitivity requirement, one can choose to combine the LFIA to electrochemical transduction or to leave the LFIA test unchanged. Our approach has the potential to be applied to all the AuNPs-based LFIA that accounts for almost 80% of the LFIA commercially available. The performance of the electrochemical methods might represent a step forward to obtain more quantitative tests. However, this should not be synonymous with more-complex and time-consuming setup: the combination of LFIA, electrochemistry, paper-based fabrication, smartphone-based reader, and nanomaterials might lead toward the development of a novel class of ASSURED diagnostics, easily extendible to other fields, i.e., environmental, pharmaceutical, agri-food.

■ ASSOCIATED CONTENT

Supporting Information

The Supporting Information is available free of charge at https://pubs.acs.org/doi/10.1021/acs.analchem.3c04078.

UV−vis spectrum and TEM image of synthesized AuNPs (Figure S1), result of flocculation stress test performed to define amount of anti-PSA mAb to be adsorbed onto AuNPs (Figure S2), fine-tuning of the test line concentration (Figure S3), and optimization of open circuit time and deposition time of voltametric detection (Figure S4) (PDF)

■ AUTHOR INFORMATION

Corresponding Authors

Fabio Di Nardo − *Department of Chemistry, Università degli Studi di Torino, 10124 Turin, Italy;* orcid.org/0000-0003-0497-4251; Email: fabio.dinardo@unito.it

Stefano Cinti − *Department of Pharmacy, University of Naples "Federico II", 80131 Naples, Italy;* orcid.org/0000-0002-8274-7452; Email: stefano.cinti@unina.it

Authors

Antonella Miglione − *Department of Pharmacy, University of Naples "Federico II", 80131 Naples, Italy*

Simone Cavalera − *Department of Chemistry, Università degli Studi di Torino, 10124 Turin, Italy*

Thea Serra − *Department of Chemistry, Università degli Studi di Torino, 10124 Turin, Italy*

Claudio Baggiani − *Department of Chemistry, Università degli Studi di Torino, 10124 Turin, Italy*

Laura Anfossi − *Department of Chemistry, Università degli Studi di Torino, 10124 Turin, Italy;* orcid.org/0000-0002-2920-0140

Complete contact information is available at: https://pubs.acs.org/10.1021/acs.analchem.3c04078

Author Contributions

All authors have given approval to the final manuscript.

Notes

The authors declare no competing financial interest.

■ ACKNOWLEDGMENTS

The research leading to these results has received funding from AIRC under MFAG 2022 - ID. 27586 project, P.I. Cinti Stefano. The authors also acknowledge support from the Project CH4.0 under the MUR program "Dipartimenti di Eccellenza 2023−2027" (CUP: D13C22003520001). The authors acknowledge the Ministry of Education, University and Research of Italy (PRIN: 2017Y2PAB8), for financial support.

■ REFERENCES

(1) Kettler, H.; White, K.; Hawkes, S. J. Mapping the Landscape of Diagnostics for Sexually Transmitted Infections: Key Findings and Recommendations. *World Health Organization*. https://apps.who.int/iris/handle/10665/68990 (accessed 2023−08−30).

(2) Land, K. J.; Boeras, D. I.; Chen, X.-S.; Ramsay, A. R.; Peeling, R. W. *Nat. Microbiol* **2019**, *4* (1), 46−54.

(3) Vazquez, M.; Anfossi, L.; Ben-Yoav, H.; Dieguez, L.; Karopka, T.; Della Ventura, B.; Abalde-Cela, S.; Minopoli, A.; Di Nardo, F.; Shukla, V. K.; Teixeira, A.; Tvarijonaviciute, A.; Franco-Martinez, L. *Lab Chip* **2021**, *21* (22), 4330−4351.

(4) Liu, Y.; Zhan, L.; Qin, Z.; Sackrison, J.; Bischof, J. C. *ACS Nano* **2021**, *15* (3), 3593−3611.

(5) Rodríguez, M. O.; Covián, L. B.; García, A. C.; Blanco-López, M. C. *Talanta* **2016**, *148*, 272−278.

(6) Li, K.; Li, X.; Fan, Y.; Yang, C.; Lv, X. *Sens. Actuators, B* **2019**, *286*, 272−281.

(7) Sciutto, G.; Zangheri, M.; Anfossi, L.; Guardigli, M.; Prati, S.; Mirasoli, M.; Di Nardo, F.; Baggiani, C.; Mazzeo, R.; Roda, A. *Angew. Chem., Int. Ed.* **2018**, *57* (25), 7385−7389.

(8) Blanco-Covián, L.; Montes-García, V.; Girard, A.; Fernández-Abedul, M. T.; Pérez-Juste, J.; Pastoriza-Santos, I.; Faulds, K.; Graham, D.; Blanco-López, M. C. *Nanoscale* **2017**, *9* (5), 2051−2058.

(9) Wang, Y.; Qin, Z.; Boulware, D. R.; Pritt, B. S.; Sloan, L. M.; González, I. J.; Bell, D.; Rees-Channer, R. R.; Chiodini, P.; Chan, W. C. W.; Bischof, J. C. *Anal. Chem.* **2016**, *88* (23), 11774−11782.

(10) Faheem, A.; Cinti, S. *Biosens. Bioelectron.* **2022**, *200*, No. 113904.

(11) Raucci, A.; Miglione, A.; Spinelli, M.; Amoresano, A.; Cinti, S. *J. Electrochem. Soc.* **2022**, *169* (3), No. 037516.

(12) Di Nardo, F.; Chiarello, M.; Cavalera, S.; Baggiani, C.; Anfossi, L. *Sensors* **2021**, *21* (15), 5185.

(13) Perju, A.; Wongkaew, N. *Anal Bioanal Chem.* **2021**, *413* (22), 5535−5549.

(14) Cheng, J.; Yang, G.; Guo, J.; Liu, S.; Guo, J. *Analyst* **2022**, *147* (4), 554−570.

(15) Zou, Z.-X.; Wang, J.; Wang, H.; Li, Y.-Q.; Lin, Y. *Talanta* **2012**, *94*, 58−64.

(16) Nian, H.; Wang, J.; Wu, H.; Lo, J.-G.; Chiu, K.-H.; Pounds, J. G.; Lin, Y. *Anal. Chim. Acta* **2012**, *713*, 50−55.

(17) de la Escosura-Muniz, A.; Parolo, C.; Maran, F.; Mekoci, A. *Nanoscale* **2011**, *3* (8), 3350−3356.

(18) Occhipinti, S.; Mengozzi, G.; Oderda, M.; Zitella, A.; Molinaro, L.; Novelli, F.; Giovarelli, M.; Gontero, P. *Cancers* **2021**, *13* (14), 3570.
(19) Di Nardo, F.; Occhipinti, S.; Gontero, P.; Cavalera, S.; Chiarello, M.; Baggiani, C.; Anfossi, L. *Sens. Actuators, B* **2020**, *325*, No. 128812.
(20) Cavalera, S.; Russo, A.; Foglia, E. A.; Grazioli, S.; Colitti, B.; Rosati, S.; Nogarol, C.; Di Nardo, F.; Serra, T.; Chiarello, M.; Baggiani, C.; Pezzoni, G.; Brocchi, E.; Anfossi, L. *Talanta* **2022**, *240*, No. 123155.
(21) Raucci, A.; Miglione, A.; Lenzi, L.; Fabbri, P.; Di Tocco, J.; Massaroni, C.; Presti, D. L.; Schena, E.; Pifferi, V.; Falciola, L.; Aidli, W.; Di Natale, C.; Netti, P. A.; Woo, S. L.; Morselli, D.; Cinti, S. *Sens. Actuators, B* **2023**, *379*, No. 133178.

https://doi.org/10.1021/acs.analchem.3c04078
Anal. Chem. XXXX, XXX, XXX−XXX